Generalized parton distributions

M. Diehl

Deutsches Elektronen-Synchroton DESY, 22603 Hamburg, Germany

Summary. — These lectures give an introduction to the theory of generalized parton distributions, starting from the underlying concepts, highlighting their physical interest, and discussing the possibilities to study them experimentally.

1. – Introduction

These lectures give an introduction to the theory of generalized parton distributions (GPDs). We first review the general ideas of factorization, highlighting the similarities and differences between generalized and usual parton distributions. We then discuss which specific information about hadron structure is contained in GPDs, focusing on the nucleon spin structure and on spatial imaging of partons. We explain the relation between GPDs and transverse-momentum dependent distributions (TMDs). Finally, we give some information about the exclusive scattering processes that allow us to study GPDs in experiments. One of the attractive features of GPDs is that they are related with many other aspects of QCD. This also means that it is impossible to give a full account of the field in these lectures. We will mostly focus on basics.

The literature on GPDs is vast, and we will only occasionally cite the original papers that have brought the field forward over the last one and a half decade. Instead, we point the reader to several reviews [1, 2, 3, 4, 5] that provide a fairly comprehensive overview, each giving slightly different emphasis to the many facets of the field.

© Società Italiana di Fisica

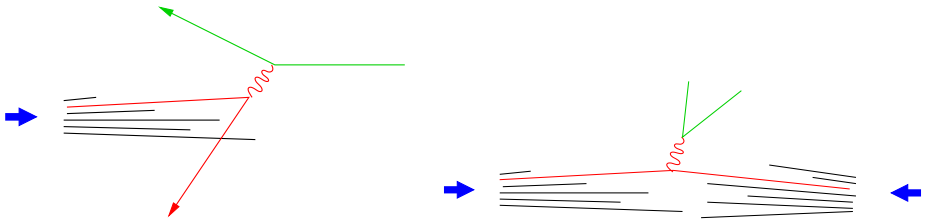

Fig. 1. – Representation of deep inelastic scattering (left) and of the Drell-Yan process (right) in the parton model. The blue arrows represent the incoming protons.

2. – Factorization in QCD

The way we think about quarks and gluons is strongly shaped by the parton model, which states that in a high-energy collision a fast moving proton behaves like a set of free partons with low transverse momenta. The cross section of a collision is then calculated from the cross section of a parton-level process (e.g. $\ell q \to \ell q$ or $\ell \bar{q} \to \ell \bar{q}$ in deep inelastic scattering, or $q\bar{q} \to \ell^+\ell^-$ in the Drell-Yan process) times the distribution function(s) to find the corresponding parton(s) in the hadron(s). The underlying physical picture is sketched in fig. 1.

The concept of factorization implements the ideas of the parton model (which is a *model*) into QCD (which is the *quantum field theory* of strong interactions) and corrects these ideas when necessary:

- it specifies the conditions (process, kinematics, observables) under which a description in terms of parton-level cross sections and parton distributions is valid
- it provides a systematic procedure for calculating corrections to the parton-model assumption that partons are free, using the perturbative expansion in α_s for the interactions between partons
- it provides a definition of parton densities that allows one to study their properties in a systematic way and, in principle, to compute them using non-perturbative methods in QCD.

2˙1. *Examples for factorization: DIS and DVCS.* – In this subsection we sketch the main steps in establishing a factorized description of a process. We will gloss over many technical details and refer the reader to [6, 7, 8] for a more careful treatment. The discussion will proceed in parallel for two example processes:

1. deep inelastic scattering (DIS), i.e. $\gamma^*(q) + p(p) \to X$, where q and p denote four-momenta. This is a fully inclusive process, to be summed over all hadronic systems X. According to the optical theorem, the cross section for this process is proportional to the imaginary part of the amplitude for Compton scattering,

$\gamma^*(q) + p(p) \to \gamma^*(q) + p(p)$. We will discuss this amplitude and only convert it into a total inclusive cross section at the very end.

2. deeply virtual Compton scattering (DVCS), i.e. $\gamma^*(q)+p(p) \to \gamma(q')+p(p')$. This is a fully exclusive process with two specified particles in the final state, and we need to calculate its amplitude. Note that in this case we have a momentum transfer between the incoming and the outgoing proton in the Compton amplitude. For DIS this transfer is zero, according to the prescription of the optical theorem.

In both cases, we are concentrating on the strong-interaction part of the physical process and have taken away the QED part, which is the radiation of a virtual photon $\gamma^*(q)$ from a lepton.

2˙1.1. Kinematics. Factorization can be established for a specified kinematical limit, which is called the Bjorken limit in DIS: $Q^2 = -q^2 \to \infty$ at fixed Bjorken scaling variable $x_B = Q^2/(2pq) = Q^2/(Q^2+W^2-m^2)$, where $W^2 = (p+q)^2$ is the square of the hadronic center-of-mass energy and m denotes the proton mass. For DVCS we extend this limit by specifying that $t = (p-p')^2$ should remain finite as $Q^2 \to \infty$; this is understood when we refer to the Bjorken limit in the following. In an experiment Q^2 is of course not infinite, and the above limit translates into the requirements that Q^2 and W^2 should be large compared with all other relevant scales (including the scale of non-perturbative QCD dynamics, which may be represented by the proton mass), and that for DVCS they should in particular be large compared with $|t|$.

To derive factorization it is convenient to work with light-cone coordinates. For any given four-vector v these are given by

$$v^+ = (v^0 + v^3)/\sqrt{2}\,, \qquad v^- = (v^0 - v^3)/\sqrt{2}\,, \tag{1}$$

and the transverse components are collected in a two-dimensional vector $\boldsymbol{v} = (v^1, v^2)$. It is easy to show([1]) that under a boost along the z axis v^+ is multiplied by a number and v^- by the inverse of that number. In particular, the ratio w^+/v^+ of two plus-components is invariant under such a boost. It is also easy to derive the rules of calculation

$$vw = v^+w^- + v^-w^+ - \boldsymbol{v}\boldsymbol{w}\,, \qquad d^4v = dv^+\, dv^-\, d^2\boldsymbol{v}\,. \tag{2}$$

Returning to our two processes, we now choose a reference frame in which the incoming proton moves fast to the right, so that p^+ is large (of order Q), p^- is very small (of order m^2/Q) and $\boldsymbol{p} = \boldsymbol{0}$. We also require that q^- and q^+ are of order Q and that $\boldsymbol{q} = \boldsymbol{0}$. One reason why such a frame is useful is that in later stages it will allow us to neglect small momentum components compared with large ones. (A frame in which a hadron moves fast is also convenient for making contact with the physical picture of the parton model.)

([1]) Whenever we state that something is easy, the reader is encouraged to check the corresponding statement as an exercise.

It is easy to see that the $\gamma^* p$ center-of-mass is an example of such a frame if the z axis is chosen along the proton momentum p. With a little more work, one also finds that the requirement of small t for DVCS translates into $p'^+ \sim q'^- \sim Q$, $p'^- \sim q'^+ \sim m^2/Q$ and $|\boldsymbol{p}'| = |\boldsymbol{q}'| \sim m$, i.e. the outgoing proton moves fast to the right and the produced real photon fast to the left.

2˙1.2. Dominant momentum regions. The next step is to consider all possible graphs for the process under study, i.e. for Compton scattering in our case. For simplicity we restrict ourselves to the light quarks (u, d, s) in the following; the inclusion of heavy quarks into the factorization formalism is possible but involves a number of complications. According to a general analysis by Libby and Sterman [9], which uses rather advanced methods of quantum field theory, the dominant contribution to any graph in the kinematic limit we are taking comes from a limited set of regions for the loop momenta:

1. *hard* momenta with $k^+ \sim k^- \sim |\boldsymbol{k}| \sim Q$, which are far off shell, $|k^2| \sim Q^2$,

2. momenta that are approximately *collinear* to one of the external hadrons and are weakly off shell, $|k^2| \sim m^2$. In DIS this means that the corresponding lines move fast to the right, $k^+ \sim Q$, $k^- \sim m^2/Q$ and $|\boldsymbol{k}| \sim m$. For DVCS there is an additional complication: since the final-state photon is real it can split into almost collinear partons (thus acting quite like a hadron), so that loop momenta may also correspond to particles moving fast to the left.

3. momenta that are *soft*, having momentum components k^+, k^- and $|\boldsymbol{k}|$ much smaller than Q. How small exactly these components are requires more discussion, and we shall gloss over this issue here.

According to these criteria, one can organize any graph into hard, collinear and soft subgraphs in the region where it gives the dominant contribution to the amplitude we want to calculate. Note that for a given graph there may be several possibilities to organize it into subgraphs, corresponding to distinct regions of the loop momenta. Some examples for this are shown in fig. 2.

2˙1.3. Power counting. Not all of the graphs selected by the Libby-Sterman criterion actually give dominant contributions to the amplitude, and a further selection is possible using power counting. This means that one determines how a given graph scales with m and Q, which can be done in a very general manner.

1. By construction, a hard subgraph involves only the large scale Q and not the small scale m. It therefore behaves like Q raised to a power that is given by the mass dimension of the subgraph. Note the elegance of this argument: it allows us to make a statement about an infinite number of subgraphs with specified external lines (which is enough to fix the mass dimension) without calculating them, and the actual mass dimension can be determined by choosing a conveniently simple graph. Figure 3 shows a few examples.

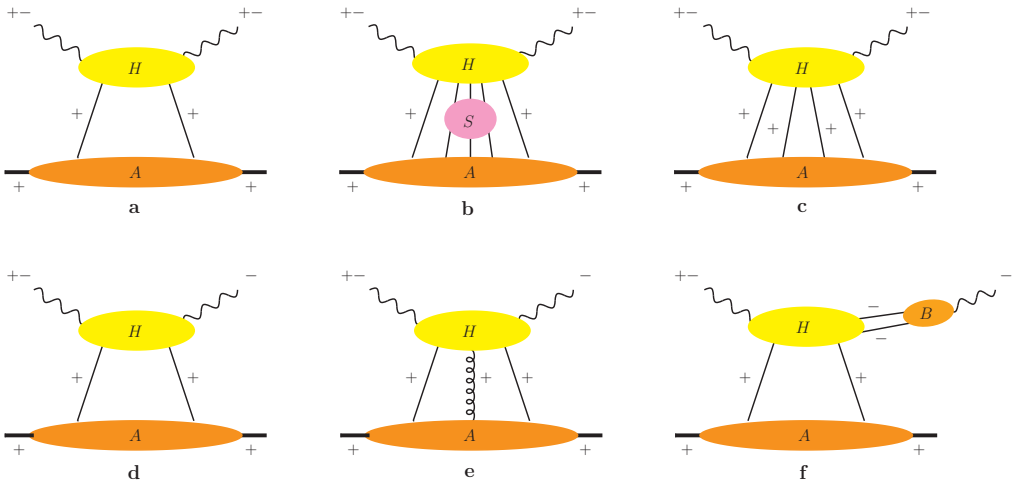

Fig. 2. – Examples of graphs that can give leading contributions to DIS (top row) and to DVCS (bottom row) according to the Libby-Sterman analysis. A + (−) next to a line indicates that it has a plus (minus) momentum of order Q. Hard subgraphs are denoted by H, soft subgraphs by S, and subgraphs collinear to the proton by A. In the case of DVCS one can also have a subgraph B collinear to the outgoing photon.

2. A somewhat more involved (but still very general) argument allows one to determine the power behavior of collinear subgraphs. One finds that for each external quark or antiquark a collinear subgraph can give at most a power $Q^{1/2}$. For each right-moving external gluon one gets a power Q if the gluon polarization vector points in the plus-direction, no power of Q if the gluon polarization is transverse, and a power of $1/Q$ if it points in the minus-direction. For left-moving gluons one has an analogous statement.

3. The integration measure for a collinear line is easily found to scale as $d^4k = dk^+\, dk^-\, d^2\boldsymbol{k} \sim m^4$.

4. The scaling behavior of soft subgraphs and of their integration measure can also be determined. It depends on the exact scaling of the soft momentum components but can never give a positive power of Q.

From points 1. and 2. we can deduce the important rule that the dominant graphs are those that have the smallest possible number of external partons in the hard subgraph: additional external partons lead to a suppression from more hard propagators that cannot be counterbalanced by the extra powers of Q from the collinear subgraphs. In fig. 2 this selection leaves us with graphs a and d.

The only exception to the rule just stated is that one can add an arbitrary number of right-moving gluons with polarization in the plus-direction (and of left-moving gluons with polarization in the minus-direction if the process involves a left-moving hadron). To

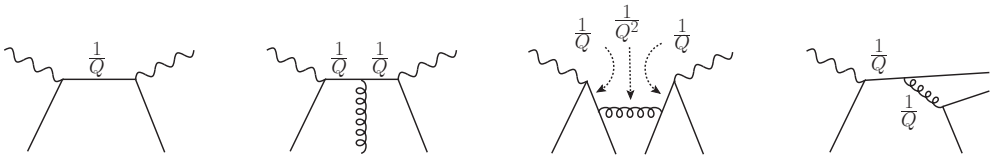

Fig. 3. – Examples of hard subgraphs (corresponding to those in fig. 2) and their power behavior in Q. The $1/Q$ and $1/Q^2$ factors correspond to the different mass dimensions of fermion and boson propagators. Note that propagators for external lines are not included in a hard graph.

have such an infinity of graphs sounds like disaster for practical calculations. Luckily, a Ward identity (which reflects the gauge invariance of QCD) allows one to cast all those graphs into a form with no extra gluons in the hard subgraph and a Wilson line operator multiplying the collinear subgraph. In these lectures I will not further discuss this issue (which is of much greater importance for TMDs than for GPDs).

The leading graphs for Compton scattering do not involve any soft subgraphs. Let me mention that soft subgraphs can appear in the leading result for processes with more than one hadron in either the initial or the final state, such as semi-inclusive DIS (SIDIS) or Drell-Yan lepton pair production. The treatment of soft subgraphs in such situations is quite nontrivial and often constitutes the most difficult part in establishing a factorization formula for the process.

2˙1.4. Collinear expansion. We have achieved a significant simplification by identifying a relatively small subset of graphs that are relevant in the kinematic limit we are interested in. For DIS and DVCS these are respectively graphs a and d in fig. 2, plus corresponding graphs where gluons instead of quarks are exchanged between the collinear and hard subgraphs. We can simplify even more by neglecting small momentum components compared with large ones when evaluating the hard subgraph $H(k)$, where k denotes the momentum of one of the incoming partons (the other one being fixed by momentum conservation). More precisely, we make a Taylor expansion

$$H(k^+, k^-, \boldsymbol{k}) = H(k^+, 0, \boldsymbol{0}) + \boldsymbol{k} \left[\frac{\partial}{\partial \boldsymbol{k}} H(k^+, 0, \boldsymbol{k}) \right]_{\boldsymbol{k}=\boldsymbol{0}} + \mathcal{O}(m^2) \,. \tag{3}$$

From the discussion in the previous subsection we can deduce that the first term in this expansion is dominant, whereas the second one comes with a relative suppression by $|\boldsymbol{k}|/Q \sim m/Q$. Retaining only the leading term, the loop integral for the complete amplitude can be simplified as

$$\int d^4k \, H(k) A(k) \approx \int dk^+ \, H(k^+ 0, \boldsymbol{0}) \Big[\int dk^- \, d^2\boldsymbol{k} \, A(k) \Big] \,. \tag{4}$$

We also neglect the light quark masses in $H(k)$. In words, the hard subgraph is now evaluated in approximate kinematics, with the incoming and outgoing partons being on

shell and strictly collinear to the proton. One therefore also speaks of the "collinear approximation". By contrast, the collinear subgraph $A(k)$ is integrated over the small minus and transverse components of the parton momentum; the corresponding integral is described by "collinear" or "integrated" parton distributions. It is very important to note that in the parton distributions we do *not* put the partons on shell and do *not* set their transverse momentum to zero. In the hard scattering, these quantities are small compared with the scale Q and can be neglected, but in the collinear factor they are as large as other relevant scales (in particular the scale of nonperturbative interactions) and are integrated over rather than set to zero.

Keeping the second term in the Taylor expansion (3), one can also calculate the $1/Q$ corrections to the amplitude, i.e. terms that vanish in the Bjorken limit. In the selection described in sect. **2**˙1.3 one then needs to keep more graphs, in particular graph e in fig. 2 with a transversely polarized gluon. For reasons explained in [10], the leading contribution in the $1/Q$ expansion is referred to as "twist two", the first subleading one as "twist three" and the $1/Q^2$ suppressed one as "twist four". Yet higher corrections are hardly ever discussed.

2˙2. *Parton distributions and hard-scattering kernels.* – The discussion so far was done in terms of Feynman graphs, which are the graphical representation for the rules of perturbation theory. For the hard subgraphs this is fine: they describe dynamics at a high scale Q, where the running coupling $\alpha_s(Q)$ is small and allows computation in successive orders of perturbation theory. However, the collinear subgraph is dominated by virtualities of order m^2 and describes nonperturbative dynamics. We therefore need a definition for the collinear subgraph that makes sense beyond perturbation theory. This is achieved by writing $\int dk^-\, d^2\boldsymbol{k}\, A(k)$ as a matrix element of quark or gluon field operators sandwiched between proton states. Since fields live in position rather than momentum space, it is useful to introduce the Fourier transform $\tilde{A}(z)$ of $A(k)$. We then have

$$\begin{aligned}\int dk^-\, d^2\boldsymbol{k}\, A(k) &= \int dk^-\, d^2\boldsymbol{k} \int \frac{d^4z}{(2\pi)^4}\, e^{ikz}\, \tilde{A}(z) \\ &= \int \frac{dz^-}{2\pi}\, e^{ik^+z^-}\, \tilde{A}(z)\Big|_{z^+=0,\boldsymbol{z}=\boldsymbol{0}}\,.\end{aligned} \tag{5}$$

An explicit example for an operator definition is

$$\begin{aligned}f_1(x) &= \frac{1}{2}\int \frac{dz^-}{2\pi}\, e^{ixp^+z^-}\, \big\langle p\big|\bar{q}(-\tfrac{1}{2}z)\,\gamma^+ W[-\tfrac{1}{2}z,\tfrac{1}{2}z]\,q(\tfrac{1}{2}z)\big|p\big\rangle\Big|_{z^+=0,\boldsymbol{z}=\boldsymbol{0}} \\ &= \begin{cases} q(x) & \text{for } x>0 \\ -\bar{q}(-x) & \text{for } x<0 \end{cases}\end{aligned} \tag{6}$$

Remember that a quark field operator q contains the annihilation operator b for a quark and the creation operator $d^\dagger$ for an antiquark. The quark density $q(x)$ thus corresponds

Fig. 4. – Handbag graphs for DIS and DVCS.

to the term $b^\dagger b$ in the product $\bar{q}\ldots q$ of fields, whereas the antiquark density $\bar{q}(-x)$ comes from the term $dd^\dagger = -d^\dagger d$, with an overall minus sign reflecting that fermion fields anticommute. W is the Wilson line operator announced in sect. **2**˙1.3 and will not be further discussed here.

A generalized parton distribution is defined in the same way as in (6), with the only difference that the proton states in the bra and the ket are not identical and have different momenta (and possibly different spin orientations).

Consider now the hard subgraphs for DIS and DVCS at leading order in the strong coupling. The Compton amplitude is then given by the so-called "handbag diagrams" shown in fig. 4. Let me not calculate these graphs in detail but rather give the answer and discuss some of its most important features.

For both DIS and DVCS the expression of the hard-scattering graph is, up to global factors, given by the propagator of the horizontal quark or antiquark line in the figure. For the graph on the left, the denominator of this propagator is $(k+q)^2 + i\epsilon$, where $i\epsilon$ is Feynman's prescription for treating the propagator pole. Using the collinear approximation (4) we have $(k+q)^2 + i\epsilon \approx 2(k^+ + q^+)q^- + i\epsilon$. One easily finds that $q^+/p^+ = -x_B$ in the Bjorken limit. Defining the plus-momentum fraction $x = k^+/p^+$ of the quark line, we obtain a hard-scattering kernel proportional to

$$\frac{1}{x - x_B + i\varepsilon} = \mathrm{PV}\,\frac{1}{x - x_B} - i\pi\delta(x - x_B) \tag{7}$$

for the graph on the left in fig. 4, where PV denotes Cauchy's principal value prescription. Putting together all global factors, we obtain the DIS cross section

$$\sigma_{\mathrm{tot}}(\gamma^* p \to X) \propto \mathrm{Im}\,\mathcal{A}(\gamma^* p \to \gamma^* p) = \pi \sum_q (e e_q)^2 \big[q(x_B) + \bar{q}(x_B)\big]\,, \tag{8}$$

where e is the positron charge and ee_q the charge of the quark. The term with $q(x_B)$ comes from the graph on the left and the term with $\bar{q}(x_B)$ from the graph on the right in fig. 4. For DVCS we are interested in both the real and imaginary part of the amplitude and schematically have

$$\mathcal{A}(\gamma^* p \to \gamma p) = \sum_q (e e_q)^2 \left[\mathrm{PV}\int dx\, \frac{\mathrm{GPD}(x, x_B, t)}{x_B - x} + i\pi\, \mathrm{GPD}(x_B, x_B, t)\right] + \ldots\,, \tag{9}$$

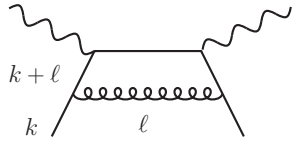

Fig. 5. – A higher-order graph for the hard scattering subprocess in DIS and DVCS.

where the contribution from the graph on the right is denoted by an ellipsis. Note that we have glossed over the spin degrees of freedom in (8) and (9). For DVCS this will be repaired in sect. **4**˙2. For DIS on an unpolarized proton (8) is the complete answer at leading order in α_s.

2˙3. *Loop corrections and evolution.* – When one calculates hard subgraphs at higher order in α_s, a complication arises which we will briefly discuss now. Take the graph in fig. 5 as an example. When the momentum ℓ becomes collinear to k the transverse part of the loop integral diverges like $\int d\boldsymbol{\ell}^2/\boldsymbol{\ell}^2$ at its lower end. A naive calculation of the hard subgraph would thus give an infinite result. But at this point we should realize that the hard subgraph is not meant to include the momentum configuration where ℓ (and hence $k+\ell$) is collinear to k: this configuration should be part of the collinear subgraph and not of the hard one.

To obtain a proper factorization formula, we must thus associate the graph at the top of fig. 6 with two different configurations: if the gluon with momentum ℓ is collinear to k then it belongs into the collinear subgraph, otherwise it goes into the hard subgraph. To implement this, one needs a so-called factorization scale μ, which is used to separate

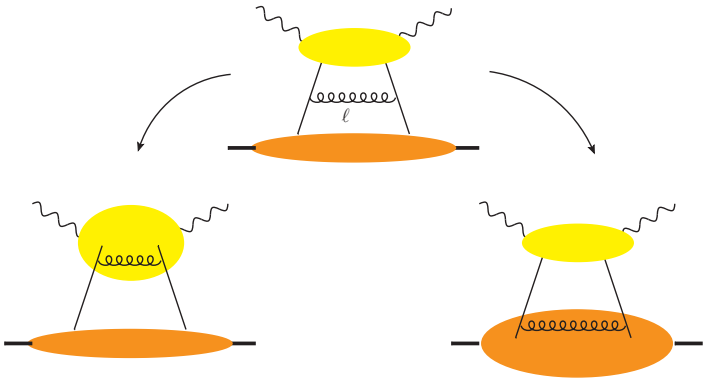

Fig. 6. – Factorization at higher order for DIS or DVCS. Depending on its momentum, the gluon in the top graph belongs either to the hard subgraph (bottom left) or to the collinear one (bottom right).

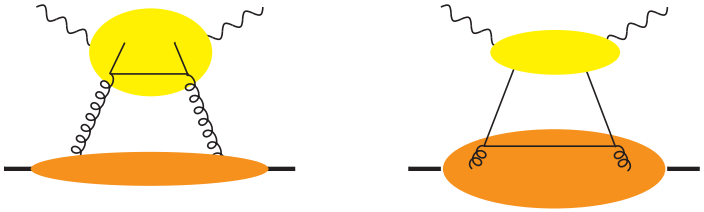

Fig. 7. – Graphs showing the interplay of quark and gluon distributions under scale evolution.

the two regions. One could then calculate the hard subgraph with $\boldsymbol{\ell}^2 > \mu^2$ (avoiding the collinear divergence mentioned above) and, at the same time, require that in the collinear subgraph this gluon should have $\boldsymbol{\ell}^2 < \mu^2$ (which avoids an ultraviolet divergence that would otherwise appear). In this way, both the hard-scattering amplitude and the parton distribution become μ dependent. In practice one does not calculate with a cutoff, which has undesirable properties such as breaking Lorentz and gauge invariance, resorting instead to a mathematical trick called dimensional regularization, which we will not further explain here. In physical terms, one may say that we use the scale μ to separate the "structure" of the proton in terms of partons (described by the parton distribution) and the "interaction" of a parton (described by the hard scattering). One can also think of $1/\mu$ as the scale in transverse configuration space at which the target structure is resolved by the hard-scattering process.

The μ dependence of the parton distribution can be described by a differential equation, which goes under the name of DGLAP evolution equation for the case of ordinary parton distributions. In the overall cross section, the dependence on the arbitrary separation scale μ should cancel, and indeed it would if one could compute the hard scattering to all orders in α_s. This one can unfortunately not do, and one finds that when the perturbative series for the hard scattering is calculated to some order α_s^n one retains a residual μ dependence in the physical cross section of order α_s^{n+1}, i.e. at an order that is beyond the accuracy of the calculation. One often uses this effect and varies μ by some factor, say between $1/2$ and 2, to estimate the size of uncalculated higher-order corrections. Within such a factor, μ should be taken of order Q; otherwise the perturbative expansion of the hard scattering has a poor convergence due to large logarithms of μ/Q. From a physics point of view this is not surprising: a hard scattering process at momentum scale Q is able to resolve the proton structure with a spatial resolution of order $1/\mu \sim 1/Q$.

Figure 6 describes the radiation of a gluon from a quark that subsequently undergoes a hard scattering. Similarly, a gluon can split into a $q\bar{q}$ pair as shown in fig. 7. This implies that as one changes the scale μ, quark and gluon distributions communicate with each other; one says that they "mix" under evolution.

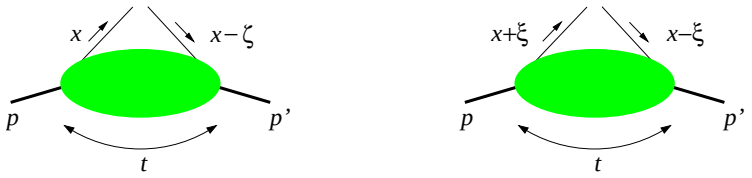

Fig. 8. – Kinematical variables describing a GPD. In the left graph plus-momentum fractions refer to p and in the right graph they refer to $P = \frac{1}{2}(p + p')$. In DVCS one has $\zeta = x_B$ and $\xi = x_B/(2 - x_B)$ in terms of the Bjorken variable.

3. – Properties and physics of GPDs

We have seen how generalized parton distributions arise in the description of hard exclusive scattering processes on the proton. Let us now take a closer look at these distributions themselves. In close analogy to the forward matrix element (6), which describes the usual quark and antiquark densities, we have

$$(10) \qquad F^q = \frac{1}{2} \int \frac{dz^-}{2\pi}\, e^{ixP^+z^-} \left\langle p', s' \middle| \bar{q}(-\tfrac{1}{2}z)\, \gamma^+ W[-\tfrac{1}{2}z, \tfrac{1}{2}z]\, q(\tfrac{1}{2}z) \middle| p, s \right\rangle \Big|_{z^+=0, \boldsymbol{z}=\boldsymbol{0}}$$
$$= H^q(x,\xi,t)\, \frac{\bar{u}(p',s')\, \gamma^+ u(p,s)}{2P^+} + E^q(x,\xi,t)\, \frac{i}{2m}\, \bar{u}(p',s')\, \frac{\sigma^{+\alpha}\Delta_\alpha}{2P^+}\, u(p,s)\,,$$

where $\Delta = p' - p$ is the momentum transfer to the proton.

Note that there are two common choices of kinematical variables for GPDs in the literature, as shown in fig. 8. The one on the left-hand side (going back to Radyushkin [11]) defines plus-momentum fractions w.r.t. the incoming proton and is the one we used in sect. **2**˙2. The one on the right (due to Ji [1]) is used in (10) and treats the two protons and the two quark lines in a symmetric way: x is the average plus-momentum of the two quark lines with respect to the average proton momentum $P = \frac{1}{2}(p + p')$, and the so-called skewness variable $\xi = (p - p')^+/(p + p')^+$ quantifies the plus-momentum loss of the proton. In both parameterizations one has the squared invariant momentum transfer $t = \Delta^2$ as a third variable. Note that the GPDs H^q and E^q additionally depend on the factorization scale μ as discussed in the previous section; this dependence will not be explicitly written in the following.

We have already seen that the forward matrix element (6) describes either a quark or an antiquark distribution, depending on the sign of x, which determines the relevant combination of creation and annihilation operators of the field product $\bar{q} \ldots q$. Repeating the same argument for (10) one finds that there are three distinct regions, as illustrated in fig. 9. The regions $\xi < x < 1$ and $-1 < x < -\xi$ are the respective analogs to the regions of positive and negative x for the parton densities. They are also called DGLAP regions, because the evolution equation for the μ dependence in these regions is very similar to the usual DGLAP evolution equation for parton densities. The central region

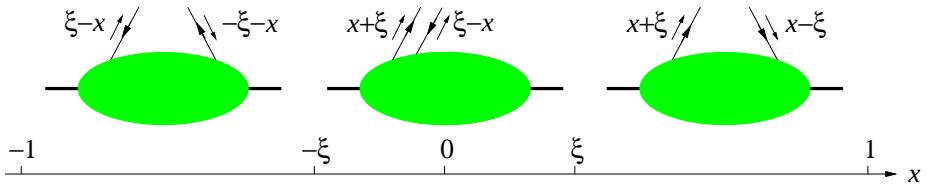

Fig. 9. – Partonic interpretation of a GPD in different regions of x. For $|x| > 1$ the matrix element in (10) is zero.

$-\xi < x < \xi$ has no analog in parton densities and describes the coherent emission of a $q\bar{q}$ pair. It has been baptized ERBL region, since the evolution equation in this case is a generalization of the ERBL evolution equation, which describes the scale dependence of a meson distribution amplitude (i.e. of the amplitude for a meson to fluctuate into a $q\bar{q}$ pair and nothing else). The realization that the apparently so different DGLAP and ERBL equations are closely connected was one of several aspects that led to the discovery of the GPD concept [12].

It is instructive to represent the GPDs in terms of the wave functions for the two proton states $\langle p'|$ and $|p\rangle$. In the DGLAP region with $x > \xi$ one then obtains a product $\psi^*_{x+\xi}\,\psi_{x-\xi}$ of wave functions for different momentum fractions $x+\xi$ and $x-\xi$ of the quark, which may be regarded as an interference term between different parton configurations of the proton. In the usual parton densities one has instead a squared wave function $|\psi_x|^2$ and can hence interpret the distribution as the probability density to find a quark with momentum fraction x.

Given the finite momentum transfer to the proton (and thus also to the parton) GPDs depend on more kinematic variables than usual parton densities. They also have a richer spin structure, because the spin orientations s' and s of the two proton states in (10) need not be the same, which reflects that in an exclusive scattering process the polarization of the outgoing proton may differ from the one of the incoming proton. In (10) the spin dependence of the matrix element is parameterized by two GPDs H^q and E^q, which are multiplied by suitable products involving the proton spinors $\bar{u}(p', s')$ and $u(p, s)$.

It is easy to see that if we set $p = p'$ in (10) then the factor multiplying H^q reduces to unity, whereas E^q is multiplied by zero. This means that H^q becomes equal to $f_1(x)$ for $\xi = 0$ and $t = 0$, so that the usual quark and antiquark densities are boundary values of the GPD H^q. By contrast, no information on E^q can be obtained from usual parton densities. Evaluating the spinor products in (10) for nonzero ξ and t and for definite helicities $\lambda, \lambda' = \pm 1$ of the proton states, one obtains

$$F^q_{\lambda=\lambda'} \propto H^q - \frac{\xi^2}{1-\xi^2}\,E^q\,, \qquad\qquad F^q_{\lambda\neq\lambda'} \propto e^{\lambda i\varphi}\,\frac{|\boldsymbol{\Delta}|}{2m}\,E^q\,, \tag{11}$$

where φ is the azimuthal angle of the transverse momentum transfer $\boldsymbol{\Delta}$. From ordinary quantum mechanics we recall that the operator for orbital angular momentum L^z along

the z axis is $-i\partial/\partial\varphi$. The exponential $e^{\lambda i\varphi}$ thus indicates that the proton helicity flip matrix element $F^q_{\lambda\neq\lambda'}$ involves one unit of orbital angular momentum, as is necessary for conserving the total angular momentum J^z along z. More explicitly, one can write this matrix element as the interference of wave functions with different orbital angular momentum [13]. This one of several ways to see that E^q is intimately related with orbital angular momentum.

The operator $\bar q(-\frac{1}{2}z)\,\gamma^+ q(\frac{1}{2}z)$ in (10) projects onto unpolarized quarks. For longitudinal quark polarization one defines

$$\begin{aligned}(12)\qquad \tilde F^q &= \frac{1}{2}\int\frac{dz^-}{2\pi}\,e^{ixP^+z^-}\,\big\langle p',s'\big|\bar q(-\tfrac{1}{2}z)\,\gamma^+\gamma_5\,W[-\tfrac{1}{2}z,\tfrac{1}{2}z]\,q(\tfrac{1}{2}z)\big|p,s\big\rangle\Big|_{z^+=0,\boldsymbol{z}=\boldsymbol{0}}\\ &= \tilde H^q(x,\xi,t)\,\frac{\bar u(p',s')\,\gamma^+\gamma_5\,u(p,s)}{2P^+} + \tilde E^q(x,\xi,t)\,\frac{1}{2m}\,\bar u(p',s')\,\frac{\gamma_5\Delta^+}{2P^+}\,u(p,s)\,.\end{aligned}$$

For $p=p'$ the distribution $\tilde H^q$ reduces to the distribution $\Delta q(x)$ of polarized quarks if $x>0$ and to the distribution $\Delta\bar q(-x)$ of polarized antiquarks if $x<0$. Since $\tilde E^q$ is multiplied by $\Delta^+/(2P^+)=-\xi$ in (12), it becomes invisible in the forward limit, just as E^q. Similar matrix elements and GPDs can be written down for transversely polarized quarks, and for unpolarized or polarized gluons.

3˙1. *Sum rules.* – We have emphasized several times the close connection between GPDs and ordinary parton densities. Let us now investigate another important connection: the one between GPDs and form factors. We easily see that, if we integrate the matrix element in (10) over x, the exponential turns into a δ function, $\int dx\,e^{ixP^+z^-}\propto\delta(z^-)$. This means that we go from the nonlocal operator $\bar q(-\frac{1}{2}z)\,\gamma^+W[-\frac{1}{2}z,\frac{1}{2}z]\,q(\frac{1}{2}z)$ to a *local* operator $\bar q(0)\,\gamma^+q(0)$, which gives the plus-component of the electromagnetic current when multiplied by the quark charge and summed over flavors. The proton matrix element of this current is parameterized by the Dirac and Pauli form factors $F_1(t)$ and $F_2(t)$, and we can thus identify

$$(13)\qquad \sum_q e_q\int_{-1}^1 dx\,H^q(x,\xi,t)=F_1(t)\,,\qquad \sum_q e_q\int_{-1}^1 dx\,E^q(x,\xi,t)=F_2(t)\,.$$

The transition from a nonlocal to a local operator in the matrix elements corresponds to the different ways in which the proton is probed in DVCS and in elastic scattering, as sketched in fig. 10.

Something remarkable has happened in (13): after integration over x, the dependence on ξ has disappeared. This is a consequence of Lorentz invariance and can be shown in a little calculation, which I will however not give here. Roughly speaking, by integrating over x we have removed the dependence of the matrix element on the particular space-time direction that was used when we defined plus and minus components in (1). The result can then no longer depend on ξ, whose definition refers to the plus-direction; only a dependence on the Lorentz invariant t is allowed.

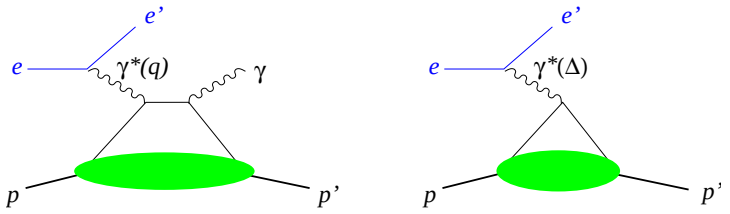

Fig. 10. – DVCS (left) probes the proton with a preferred direction, given by the γ^* momentum in the $\gamma^* p$ center-of-mass. In elastic scattering (right) the photon with its pointlike coupling to quarks is a local probe that does not single out any space-time direction.

If we take Mellin moments, i.e. integrate the matrix element in (10) over x with a weight x^n, then the exponential factor $e^{ixP^+z^-}$ turns into the nth derivative of a δ function. Letting this act on $q(-\frac{1}{2}z)\dots W[-\frac{1}{2}z,\frac{1}{2}z]\,q(\frac{1}{2}z)$ gives local operators with covariant derivatives $\partial^+ + igA^+(0)$ between the quark fields $\bar{q}(0)$ and $q(0)$. For the derivative part ∂^+ this is easy to see, and with a bit more work one finds that the gluon potential part comes from taking the derivative of the Wilson line operator $W[-\frac{1}{2}z,\frac{1}{2}z]$. One also finds that Lorentz invariance restricts the possible dependence on ξ of the result to be a polynomial of a specific order,

$$\int_{-1}^{1} dx\, x^{n-1} H^q(x,\xi,t) = \sum_{k=0}^{n} (2\xi)^k\, A^q_{n,k}(t)\,, \qquad \int_{-1}^{1} dx\, x^{n-1} E^q(x,\xi,t) = \sum_{k=0}^{n} (2\xi)^k\, B^q_{n,k}(t)\,, \tag{14}$$

where k is even because the GPDs are even functions of ξ due to time reversal invariance. The constraint in (14) is called *polynomiality*, and the absence of ξ dependence in (13) is a special case of it (with polynomials of degree zero). Note that this property requires a delicate interplay between the DGLAP and ERBL regions under the integral: although the physical interpretation of these regions is very different, Lorentz invariance ties them together in a way that is not easy to grasp for our intuition. On a more practical side, ensuring polynomiality (and hence Lorenz invariance) is an important criterion to fulfill when one writes down models for GPDs. Two of the most widely used approaches satisfy this criterion by construction, namely the ansatz using double distributions described in [14, 2] and the ansatz using conformal moments in [15, 16].

The Mellin moments with $n = 2$ in (14) play a particular role. The are matrix elements of the quark part of the energy-momentum tensor. For the sum $H^q + E^q$ one finds the celebrated sum rule of Ji [17]:

$$\frac{1}{2}\int_{-1}^{1} dx\, x\big[H^q(x,\xi,t) + E^q(x,\xi,t)\big] = \frac{1}{2}\big[A^q_{2,0}(t) + B^q_{2,0}(t)\big] = J^q(t)\,, \tag{15}$$

where $J^q(0)$ gives the *total* angular momentum carried by quarks and antiquarks of flavor q in the proton, including both their helicity and their orbital motion. Whereas a wealth of inclusive processes with polarized targets allows us to measure the helicity of partons, probing their orbital angular momentum is much more difficult, and Ji's sum rule offers a rare chance to do this. A relation analogous to (15) exists for gluon GPDs and $J^g(t)$. The attentive reader will have noticed that there is no term going with ξ^2 in (15), unlike in the general formula (14). The reason is that for the highest coefficients there one has $A^q_{n,n}(t) + B^q_{n,n}(t) = 0$.

Notice finally that matrix elements of local operators are suitable for evaluation in Euclidean space-time. For n up to 2 the form factors in (14) have been calculated on the lattice, which provides a valuable opportunity to study aspects of GPDs in a fully nonperturbative fashion. More details on this can be found in Philipp Hägler's lectures at this school, and in the review [18].

3˙2. *Impact parameter*. – Among the most interesting aspects of GPDs is that they contain information about the spatial distribution of partons inside the proton. To quantify where the partons are, we first need to localize the proton. We do this by forming wave packets

$$|p^+, \boldsymbol{b}\rangle = \int \frac{d^2\boldsymbol{p}}{(2\pi)^2}\, e^{-i\boldsymbol{b}\boldsymbol{p}}\, |p^+, \boldsymbol{p}\rangle \tag{16}$$

centered at position $\boldsymbol{b}$ in the transverse plane, while keeping the plus-momentum of the state fixed. This allows us to discuss the localization of partons while keeping information about their longitudinal momentum. This can in particular be done in a frame where the proton moves fast, so that we can keep a parton model picture. Remarkably, the localization in two dimension is possible even in a relativistic theory, where an object cannot be localized in all three space dimensions with an accuracy better than its Compton wavelength.

The proton is an extended object itself, and closer analysis shows that the position $\boldsymbol{b}$ of the state (16) can be understood as the *center of plus-momentum* of the proton constituents,

$$\boldsymbol{b} = \frac{\sum_i p_i^+ \boldsymbol{b}_i}{\sum_i p_i^+}\,, \tag{17}$$

where the i quarks or gluons have plus-momenta p_i^+ and positions $\boldsymbol{b}_i$. This may be seen as a relativistic analog of the center of mass in nonrelativistic physics, where the weights are given by the masses m_i instead of the plus-momenta of the constituents.

Let us now consider the operator

$$\mathcal{O} = \frac{1}{2}\int \frac{dz^-}{2\pi}\, e^{ixP^+z^-}\, \bar{q}(-\tfrac{1}{2}z)\,\gamma^+ W[-\tfrac{1}{2}z, \tfrac{1}{2}z]\, q(\tfrac{1}{2}z)\,\Big|_{z^+=0, \boldsymbol{z}=\boldsymbol{0}} \tag{18}$$

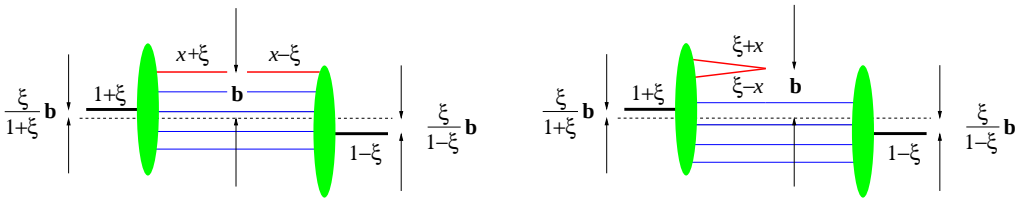

Fig. 11. – Impact parameter interpretation of a GPD in the DGLAP region (left) and in the ERBL region (right).

in (10), which describes partons localized at transverse position $\boldsymbol{z} = \boldsymbol{0}$, and take its matrix element between localized proton states, setting $p'^+ = p^+$ for simplicity. We have

$$\begin{aligned}(19)\qquad \big\langle p^+, -\boldsymbol{b}' \big| \mathcal{O} \big| p^+, -\boldsymbol{b} \big\rangle &= \int \frac{d^2\boldsymbol{p}'}{(2\pi)^2}\, \frac{d^2\boldsymbol{p}}{(2\pi)^2}\, e^{-i(\boldsymbol{b}'\boldsymbol{p}' - \boldsymbol{b}\boldsymbol{p})}\, \big\langle p^+, \boldsymbol{p}' \big| \mathcal{O} \big| p^+, \boldsymbol{p} \big\rangle \\ &= \int \frac{d^2\boldsymbol{P}}{(2\pi)^2}\, \frac{d^2\boldsymbol{\Delta}}{(2\pi)^2}\, e^{-i(\boldsymbol{b}'-\boldsymbol{b})\boldsymbol{P} - i(\boldsymbol{b}'+\boldsymbol{b})\boldsymbol{\Delta}/2}\, \big\langle p^+, \boldsymbol{p}' \big| \mathcal{O} \big| p^+, \boldsymbol{p} \big\rangle\,,\end{aligned}$$

where in the last step we have changed variables from $\boldsymbol{p}', \boldsymbol{p}$ to $\boldsymbol{P} = \frac{1}{2}(\boldsymbol{p}+\boldsymbol{p}')$, $\boldsymbol{\Delta} = \boldsymbol{p}' - \boldsymbol{p}$. On the r.h.s. we recognize the matrix element that appears in the definition (10) of GPDs. Using Lorentz invariance one can show that this matrix element depends on the difference $\boldsymbol{\Delta}$ of transverse momenta of two proton states but not on their average. We can hence carry out the integration over $\boldsymbol{P}$ and get

$$(20)\qquad \big\langle p^+, -\boldsymbol{b}' \big| \mathcal{O} \big| p^+, -\boldsymbol{b} \big\rangle = \delta^{(2)}(\boldsymbol{b}' - \boldsymbol{b}) \int \frac{d^2\boldsymbol{\Delta}}{(2\pi)^2}\, e^{-i\boldsymbol{b}\boldsymbol{\Delta}}\, \big\langle p^+, \boldsymbol{p}' \big| \mathcal{O} \big| p^+, \boldsymbol{p} \big\rangle\,.$$

Taking equal helicities for the proton states in (20) and using (10) we can identify

$$(21)\qquad q(x, \boldsymbol{b}^2) = \int \frac{d^2\boldsymbol{\Delta}}{(2\pi)^2}\, e^{-i\boldsymbol{b}\boldsymbol{\Delta}}\, H^q(x, \xi = 0, t = -\boldsymbol{\Delta}^2)$$

as the probability density to find a quark with momentum fraction x at a transverse distance $\boldsymbol{b}$ from the center of the proton [19]. One easily finds that integrating (21) over $\boldsymbol{b}$ gives back the usual quark density $q(x)$.

For nonzero skewness ξ the picture is slightly more complicated since we have no probability interpretation. Nevertheless, one finds that the Fourier transform of the GPD w.r.t. $\boldsymbol{\Delta}$ gives information about the position of the parton in the transverse plane [20]. This is shown in fig. 11. The transverse shift of the proton position is a consequence of the finite plus-momentum transfer, which changes the center of plus-momentum. Since in an exclusive process $\boldsymbol{\Delta}$ is a observable quantity, we can rather directly obtain spatial information from experiment.

3˙2.1. Transverse deformation and spin-orbit correlations. We will now see what happens with the localization of partons in the proton in the presence of polarization. For simplicity we set $\xi = 0$ again; but a similar discussion can be given for nonzero ξ. As we see in (11), the distribution E^q describes proton helicity flip. We may change basis from helicity eigenstates $|\uparrow\rangle, |\downarrow\rangle$ to states $|\pm\rangle_X = \big(|\uparrow\rangle \pm |\downarrow\rangle\big)/\sqrt{2}$, which correspond to definite spin along the positive or negative x direction. We then easily find that the helicity-flip matrix elements correspond to a polarization difference in the transverse plane:

$$ {}_X\langle +|\mathcal{O}|+\rangle_X \;-\; {}_X\langle -|\mathcal{O}|-\rangle_X = \langle\uparrow|\mathcal{O}|\downarrow\rangle + \langle\downarrow|\mathcal{O}|\uparrow\rangle \tag{22} $$

for any operator $\mathcal{O}$. Using this for the helicity-flip matrix element in (11) and taking the Fourier transform w.r.t. $\boldsymbol{\Delta}$, we find that the density of quarks in a proton polarized along the positive x direction is

$$ q_X(x,\boldsymbol{b}) = q(x,\boldsymbol{b}^2) - \frac{b^y}{m}\,\frac{\partial}{\partial \boldsymbol{b}^2}\, e^q(x,\boldsymbol{b}^2)\,, \tag{23} $$

where the Fourier transform $e^q(x,\boldsymbol{b}^2)$ of $E^q(x,\xi=0,t=-\boldsymbol{\Delta}^2)$ is defined in analogy to (21). The transverse distribution of partons is hence shifted sideways if the proton has transverse polarization. This shift is described by E^q, which thus quantifies a particular spin-orbit correlation in the proton. We know that this correlation must be sizeable at least for *some* values of x because the first moment of E^q is related with the Pauli form factor, which is known experimentally. For $t = 0$ one finds

$$ \int_{-1}^{1} dx\, E^u(x,\xi,0) \approx 1.67\,, \qquad\qquad \int_{-1}^{1} dx\, E^d(x,\xi,0) \approx -2.03\,. \tag{24} $$

How big the corresponding effects are for sea quarks and for gluons is an intriguing question and currently unknown. Let me remark that an analogous transverse shift in the spatial distribution is also obtained if the quark instead of the proton carries transverse polarization. This is quantified by transversity GPDs, which are not discussed in these lectures for reasons of space.

3˙3. *Transverse momentum vs. transverse position of partons.* – We have seen that GPDs describe the partonic structure of hadrons in transverse configuration space. Quite different information is contained in transverse-momentum dependent parton distributions (TMDs), which can be measured in semi-inclusive DIS or in Drell-Yan production. Let us take a closer look at the relation between these two types of distributions.

From ordinary quantum mechanics we are accustomed to the fact that transverse position and transverse momentum are Fourier conjugate variables. This remains true in quantum field theory, as we have already used when constructing a spatially localized proton state in (16). Likewise, we can write down a quark field operator associated with

partons of definite transverse momentum. Namely,

$$q(\boldsymbol{k}, z^-, z^+ = 0) = \int d^2\boldsymbol{z}\, e^{-i\boldsymbol{z}\boldsymbol{k}}\, q(\boldsymbol{z}, z^-, z^+ = 0) \tag{25}$$

annihilates quarks with transverse momentum $\boldsymbol{k}$ and creates antiquarks with transverse momentum $-\boldsymbol{k}$. In the matrix elements defining GPDs (as well as in those defining TMDs) we have bilinear operators. Simple algebra gives

$$\begin{aligned} \bar{q}(\boldsymbol{k'})\, q(\boldsymbol{k}) &= \int d^2\boldsymbol{z'}\, d^2\boldsymbol{z}\, e^{i(\boldsymbol{z'}\boldsymbol{k'} - \boldsymbol{z}\boldsymbol{k})}\, \bar{q}(\boldsymbol{z'})\, q(\boldsymbol{z})\,, \\ \boldsymbol{z'}\boldsymbol{k'} - \boldsymbol{z}\boldsymbol{k} &= (\boldsymbol{z'} - \boldsymbol{z})\, \frac{\boldsymbol{k'} + \boldsymbol{k}}{2} + \frac{\boldsymbol{z'} + \boldsymbol{z}}{2}\, (\boldsymbol{k'} - \boldsymbol{k})\,, \end{aligned} \tag{26}$$

where we have omitted the arguments for plus- and minus-components. We thus see that

- the average transverse momentum is Fourier conjugate to the transverse position difference and
- the transverse momentum difference is Fourier conjugate to the average transverse momentum,

where the "average" and "difference" refer to the two operators, and hence to the two parton legs in the corresponding matrix elements. Note that the average transverse momentum and position are independent variables and *not* related by a Fourier transform.

After this little exercise we can contrast the impact parameter distributions discussed in the previous subsections with TMDs. For simplicity we set $\xi = 0$ in the following and do not display longitudinal variables in the field operators and proton states. Furthermore, we use fields depending on transverse position and proton states with definite transverse momentum. In an impact parameter distribution

$$q(x, \boldsymbol{b}) \propto \int d^2\boldsymbol{\Delta}\, e^{-i\boldsymbol{b}\boldsymbol{\Delta}} \left\langle \tfrac{1}{2}\boldsymbol{\Delta} \middle| \bar{q}(\boldsymbol{0}) \ldots q(\boldsymbol{0}) \middle| -\tfrac{1}{2}\boldsymbol{\Delta} \right\rangle \tag{27}$$

we have quarks at position $\boldsymbol{0}$ and proton states at position $-\boldsymbol{b}$ (so that $\boldsymbol{b}$ is the distance of the quarks from the proton center). For a TMD we have instead quarks with transverse momentum $\boldsymbol{k}$ in a proton with transverse momentum $\boldsymbol{0}$,

$$q(x, \boldsymbol{k}) \propto \int d^2\boldsymbol{z}\, e^{-i\boldsymbol{z}\boldsymbol{k}} \left\langle \boldsymbol{0} \middle| \bar{q}(-\tfrac{1}{2}\boldsymbol{z}) \ldots q(\tfrac{1}{2}\boldsymbol{z}) \middle| \boldsymbol{0} \right\rangle. \tag{28}$$

The two functions carry different information about the proton and cannot be obtained from each other. We can however introduce GPDs that are not integrated over transverse momentum:

$$H(x, \boldsymbol{k}, \boldsymbol{\Delta}) \propto \int d^2\boldsymbol{z}\, e^{-i\boldsymbol{z}\boldsymbol{k}} \left\langle \tfrac{1}{2}\boldsymbol{\Delta} \middle| \bar{q}(-\tfrac{1}{2}\boldsymbol{z}) \ldots q(\tfrac{1}{2}\boldsymbol{z}) \middle| -\tfrac{1}{2}\boldsymbol{\Delta} \right\rangle, \tag{29}$$

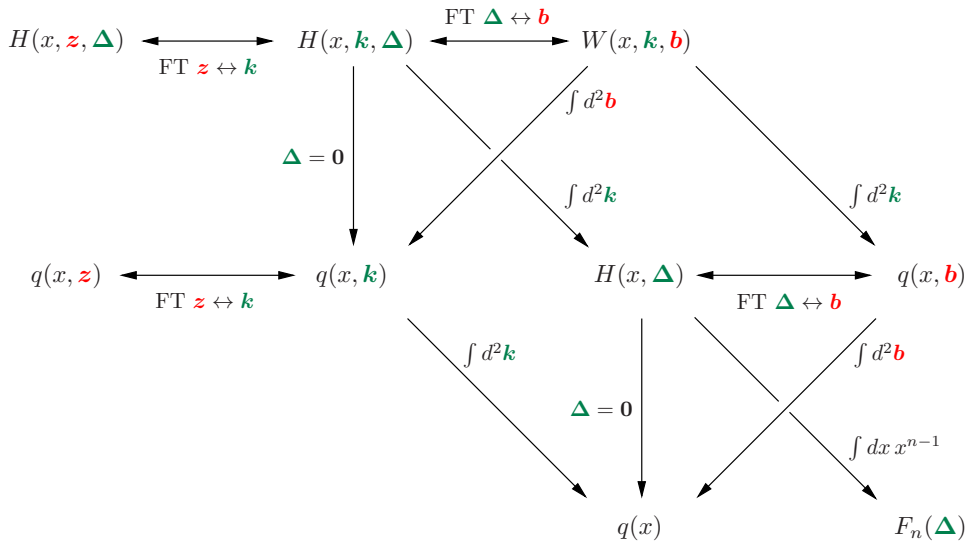

Fig. 12. – Different types of distributions and their connection with each other. GPDs and related quantities are all taken at $\xi = 0$. The form factor F_n corresponds to $A_{n,0}$ in (14).

still keeping $\xi = 0$ for simplicity. At $x > 0$ these distributions correspond to a quark leaving the proton with transverse momentum $\boldsymbol{k} - \frac{1}{2}\boldsymbol{\Delta}$ and returning with transverse momentum $\boldsymbol{k} + \frac{1}{2}\boldsymbol{\Delta}$. Fourier transforming this w.r.t. $\boldsymbol{\Delta}$ as we did with transverse-momentum integrated GPDs, we obtain a distribution

$$W(x, \boldsymbol{k}, \boldsymbol{b}) \propto \int d^2\boldsymbol{\Delta}\, d^2\boldsymbol{z}\, e^{-i\boldsymbol{b}\boldsymbol{\Delta} - i\boldsymbol{z}\boldsymbol{k}} \left\langle \tfrac{1}{2}\boldsymbol{\Delta} \middle| \bar{q}(-\tfrac{1}{2}\boldsymbol{z}) \ldots q(\tfrac{1}{2}\boldsymbol{z}) \middle| -\tfrac{1}{2}\boldsymbol{\Delta} \right\rangle \tag{30}$$

associated with transverse momentum $\boldsymbol{k}$ and transverse position $\boldsymbol{b}$ of the quark, where we must now keep in mind that both quantities are averaged over the quark legs that leave the proton and return to it. Distributions with this structure are well-known in other parts of physics and go under the name of Wigner distributions. They contain at the same time the information of impact parameter distributions and of TMDs. They can e.g. be calculated in quark models, but unfortunately we do not know how to determine them from an observable process in a model independent way.

Figure 12 gives an overview of the different types of distributions and form factors we have seen. Let me mention that the distributions on the very left depend on the relative transverse position between the two quark fields in the operator definition and are for instance useful for the resummation of Sudakov logarithms; an aspect I will not discuss here.

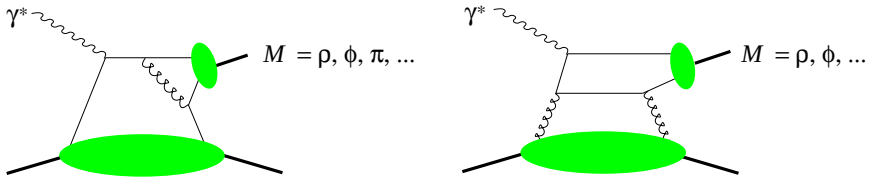

Fig. 13. – Example graphs for hard exclusive meson production, involving quark GPDs (left) or, for vector mesons, gluon GPDs (right).

4. – Studying GPDs in exclusive reactions

In sect. **2** we have used the process of deeply virtual Compton scattering, $\gamma^* p \to \gamma p$, to introduce the concept of GPDs. There are, however, more processes where the same distributions can be measured. As a "mirror process" of DVCS one may regard timelike Compton scattering (TCS), $\gamma p \to \gamma^* p$, where the initial photon is real and the final one has a timelike virtuality, whereas in DVCS the final photon is real and the initial one has a spacelike virtuality. The timelike photon in TCS decays into a lepton pair (just as in the Drell-Yan process) and the physically observed process is $\gamma p \to \ell^+ \ell^- p$. It turns out that at leading order in α_s DVCS and TCS involve exactly the same integrals over GPDs, whereas at higher orders the integrals differ [21]. Already different integrals at lowest order are involved in the description of double DVCS, $\gamma^* p \to \gamma^* p$, where the initial photon has a spacelike and the final photon a timelike virtuality. In the following we collectively refer to DVCS, TCS and double DVCS as "Compton scattering".

A large class of processes involving GPDs is the exclusive production of mesons from a virtual photon, $\gamma^* p \to M p$, where M can be a light meson such as a pion, kaon, ρ, ϕ etc. If the produced meson is made from two heavy quarks, such as a J/Ψ or an Υ, the quark mass provides a hard scale and the initial photon may also be real. Figure 13 shows example graphs for these processes. If the meson has negative charge conjugation parity $C = -1$, as is the case of vector mesons, both quark and gluon GPDs appear at lowest order in the strong coupling. These channels are therefore particularly sensitive to gluons in the proton, whereas in Compton scattering gluon GPDs only appear at the level of α_s corrections and through the scale evolution of the quark GPDs (in the same way in which the ordinary gluon distribution appears in DIS). Especially good "gluon filters" are J/Ψ and Υ production, since GPDs for heavy quarks only become relevant at very high virtualities Q of the photon (much higher than the heavy quark mass).

Using parity invariance of the hard-scattering subprocess one can show that (in the Bjorken limit) vector meson production involves the distributions H^q, E^q, H^g, E^g for unpolarized partons, whereas the production of pseudoscalar mesons is sensitive to longitudinal quark polarization in the form of $\tilde{H}^q, \tilde{E}^q$ (gluons do not contribute in this case because pseudoscalar mesons have $C = +1$). By contrast, one finds that Compton scattering involves $H^q, E^q, \tilde{H}^q, \tilde{E}^q$ at tree level and additionally the corresponding gluon GPDs at higher order. Furthermore, Compton scattering and the different meson

production channels involve different linear combinations of GPDs for the various quark flavors. It is thus the combination of many processes that will ultimately be necessary to disentangle the many GPDs, a situation well-known from the study of ordinary parton distributions.

The theory description of meson production is, however, more complicated than the one for Compton scattering. The most obvious complication is that meson production involves two types of collinear subgraphs, one for the proton and one for the meson, and correspondingly depends on two types of nonperturbative functions: GPDs for the proton and the distribution amplitude of the produced meson. Moreover, various studies find that meson production is more sensitive to corrections, both to higher orders in α_s and to power corrections in $1/Q$, see e.g. [22] and [23, 24]. A reliable theory description therefore requires larger values of Q for meson production; how large depends on the channel and is often subject of debate among theorists.

Another important difference between Compton scattering and meson production is the selection of helicities in the hard-scattering subprocess. One finds that the leading amplitude for DVCS and TCS is Q independent at fixed ξ (up to logarithmic scaling violation effects) and involves transverse photon polarization. (For double DVCS one has an additional leading amplitude with longitudinal photons, starting however only at order α_s.) By contrast, the leading amplitude for light meson production at given ξ scales like $1/Q$ up to logarithms and involves longitudinal photon and meson production. Only for J/Ψ and Υ electroproduction with Q comparable to the meson mass do we have amplitudes of similar magnitude for transverse and for longitudinal polarization of the photon and the meson.

4˙1. *From process amplitudes to GPDs.* – In sect. **2˙2** we have already seen that the amplitude for DVCS is given by an integral over GPDs times a factor describing the hard-scattering process (commonly called a hard-scattering kernel). We will now take a closer look at this. Let us first take a closer look at the spin structure. For the leading amplitudes of DVCS one can write a general decomposition

$$\begin{aligned} e^{-2}\mathcal{A}(\gamma^* p \to \gamma p) = {} & \mathcal{H}\,\frac{\bar u(p',s')\,\gamma^+ u(p,s)}{2P^+} + \mathcal{E}\,\frac{i}{2m}\,\bar u(p',s')\,\frac{\sigma^{+\alpha}\Delta_\alpha}{2P^+}\,u(p,s) \\ & + \mu\left[\tilde{\mathcal{H}}\,\frac{\bar u(p',s')\,\gamma^+\gamma_5\,u(p,s)}{2P^+} - \xi\tilde{\mathcal{E}}\,\frac{1}{2m}\,\bar u(p',s')\,\gamma_5\,u(p,s)\right], \end{aligned} \tag{31}$$

where $\mu = \pm 1$ is the helicity of the initial and final state photon. $\mathcal{H}$, $\mathcal{E}$, $\tilde{\mathcal{H}}$ and $\tilde{\mathcal{E}}$ depend on ξ, t, Q^2 and are called Compton form factors. The prefactors and proton spinor products in (31) have been chosen to match the GPD definitions (10) and (12). To leading order in α_s one has

$$\mathcal{H}(\xi,t,Q^2) = \sum_q e_q^2 \int_{-1}^{1} dx\,\frac{H^q(x,\xi,t;Q^2) - H^q(-x,\xi,t;Q^2)}{\xi - x - i\varepsilon} \tag{32}$$

where the last argument of H^q is the factorization scale, set equal to Q^2 here. Analogous relations hold for the other three GPDs. Note that the decomposition (31) remains valid at higher orders in α_s. Furthermore, one can write down similar decompositions for exclusive meson production. Using the relation (7) with x_B replaced by ξ, we see that at leading order in α_s the imaginary parts of the Compton form factors are given by GPDs at the points $x = \xi$ and $x = -\xi$, i.e. at the boundaries between the DGLAP and ERBL regions. The real parts of the form factors are given by principal value integrals over the full x interval from -1 to 1 and thus seem to depend on more details of the GPDs. However, one can prove a dispersion relation, which at leading order in α_s reads [25]

$$\begin{aligned} \text{(33)} \qquad \operatorname{Re}\mathcal{H}(\xi,t,Q^2) &= \mathrm{PV}\int_{-1}^{1} dx\, \frac{H^q(x,\xi,t;Q^2) - H^q(-x,\xi,t;Q^2)}{\xi - x} \\ &= \mathrm{PV}\int_{-1}^{1} dx\, \frac{H^q(x,x,t;Q^2) - H^q(-x,x,t;Q^2)}{\xi - x} + \mathcal{C}(t;Q^2) \end{aligned}$$

where $\mathcal{C}(t;Q^2)$ is independent of ξ and can be computed in terms of $H^q(x,\xi,t;Q^2)$. More precisely, $\mathcal{C}(t;Q^2)$ is an integral over the so-called D term first introduced in [26]. A relation analogous to (33) holds for $\mathcal{E}$ and involves $-\mathcal{C}(t;Q^2)$ instead of $\mathcal{C}(t;Q^2)$ on the r.h.s., and analogous relations for $\tilde{\mathcal{H}}$ and $\tilde{\mathcal{E}}$ do not have such a term at all [27]. Up to the quantity $\mathcal{C}(t;Q^2)$ the Compton form factors thus involve only GPDs at $x = \pm\xi$.

An important consequence of this is that a leading order analysis of Compton scattering (and likewise of any meson production channel) cannot reconstruct the full x dependence of GPDs at given ξ. Only the effects incorporated in Q^2 evolution and in the explicit higher-order corrections contain information about the GPDs away from $x = \pm\xi$. To which extent a reconstruction of the full x dependence using such effects can be achieved in realistic situations is currently not clear.

4˙2. *A closer look at DVCS.* – There is another aspect that singles out Compton scattering compared with meson production. In the following we concentrate on the DVCS process; a similar discussion can be given for TCS and for double DVCS.

Recall that DVCS is observed in elastic lepton-proton scattering, $\ell p \to \ell\gamma p$. The same reaction can take place by emitting the photon from the lepton line, as shown in fig. 14. This is the Bethe-Heitler process, where the scattering on the proton is mediated by a single photon of momentum Δ. The necessary information on the proton structure is hence described by the electromagnetic form factors $F_1(t)$ and $F_2(t)$ we already encountered in (13); since these are well-measured at low t one can calculate the Bethe-Heitler process to good precision.

The relative importance of DVCS and the Bethe-Heitler process strongly depends on kinematics, with their relative strength roughly going like

$$\text{(34)} \qquad \frac{d\sigma^C}{dx_B\, dQ^2\, dt\, d\phi} : \frac{d\sigma^{BH}}{dx_B\, dQ^2\, dt\, d\phi} \sim \frac{1}{y^2}\frac{1}{Q^2} : \frac{1}{|t|}\,,$$

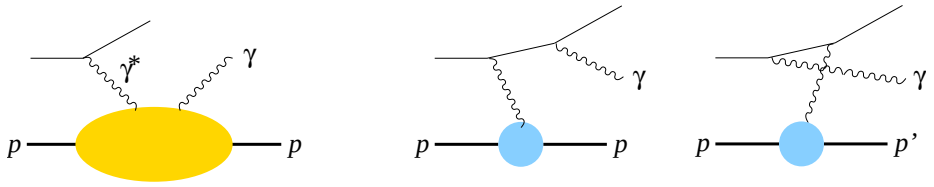

Fig. 14. – The two subprocesses contributing to the process $\ell p \to \ell \gamma p$: virtual Compton scattering (left) and the Bethe-Heitler process (right).

where the superscripts C and BH respectively stand for Compton and Bethe-Heitler. $y = Q^2/(x_B\, s_{\ell p})$ is the usual inelasticity variable in lepton-proton scattering, with $s_{\ell p}$ being the squared ℓp center-of-mass energy, and ϕ is the azimuthal angle between the plane determined by the leptons and the plane determined by the hadrons in the proton rest frame (see [28] for a precise definition). The factors $1/Q^2$ and $1/t$ in (34) respectively come from the propagators of the virtual photons in DVCS and the Bethe-Heitler process, and the factor $1/y^2$ comes from the lepton-photon vertex in DVCS. The two subprocesses interfere at the amplitude level, and the size of their interference term $d\sigma^I/(dx_B\, dQ^2\, dt\, d\phi)$ is typically in-between the two contributions in (34).

Since the validity of factorization for DVCS requires $|t|$ to be small compared with Q^2, the Bethe-Heitler process is typically more important, except for small y. However, even if y is not small, one can extract information about Compton scattering from the DVCS-Bethe-Heitler interference. This actually provides a unique chance: since the Bethe-Heitler process amplitude can be computed, the interference term allows one to measure not only size of the DVCS amplitude but also its *phase*. In other words, it gives separate information about the real and imaginary parts of the Compton form factors.

To "filter out" the interference term in the ℓp cross section one can make use of several asymmetries. As is evident from fig. 14 the DVCS contribution to the ℓp amplitude contains a single lepton-photon vertex and thus changes sign if one switches from a negative to a positive lepton beam. By contrast, the Bethe-Heitler amplitude contains two lepton-photon vertices and is independent of the lepton charge $e_\ell = \pm 1$. The interference term is therefore linear in e_ℓ and can be separated by measuring the beam charge asymmetry.

A different way of separating the different contributions makes use of the polarization of the initial lepton or the initial proton. Using the invariance of strong and electromagnetic interactions under parity and time reversal, one can show that a single spin asymmetry (either w.r.t. the lepton or to the proton) does not receive any contribution from the Bethe-Heitler process by itself, leaving one with the interference term and the

pure DVCS contribution. In full glory one has

$$
\begin{aligned}
(35) \qquad d\sigma(\ell p \to \ell\gamma p) \sim\ & d\sigma_{UU}^{BH} && + e_\ell\, d\sigma_{UU}^{I} && + d\sigma_{UU}^{C} \\
& + P_\ell S_L\, d\sigma_{LL}^{BH} && + e_\ell P_\ell S_L\, d\sigma_{LL}^{I} && + P_\ell S_L\, d\sigma_{LL}^{C} \\
& + P_\ell S_T\, d\sigma_{LT}^{BH} && + e_\ell P_\ell S_T\, d\sigma_{LT}^{I} && + P_\ell S_T\, d\sigma_{LT}^{C} \\
& && + e_\ell P_\ell\, d\sigma_{LU}^{I} && + P_\ell\, d\sigma_{LU}^{C} \\
& && + e_\ell S_L\, d\sigma_{UL}^{I} && + S_L\, d\sigma_{UL}^{C} \\
& && + e_\ell S_T\, d\sigma_{UT}^{I} && + S_T\, d\sigma_{UT}^{C}\,,
\end{aligned}
$$

where the first subscript U, L in $d\sigma$ indicates an unpolarized or longitudinally polarized lepton beam and the second subscript U, L, T an unpolarized, longitudinally or transversely polarized proton target. P_ℓ is the lepton beam polarization, and S_L, S_T denote the longitudinal and transverse proton polarizations. For a transversely polarized proton, one has in addition a dependence on the azimuthal angle ϕ_S between the lepton plane and the target spin in the proton rest frame (see [28]). As announced, there is no Bethe-Heitler contribution to the single spin terms LU, UL and UT in (35). Using parity invariance, one can further show that the single spin terms are odd under the simultaneous replacement $\phi \to -\phi$ and $\phi_S \to -\phi_S$, whereas the unpolarized or double spin terms UU, LL and LT are even under that replacement.

The interference terms contain information about the phase of the Compton amplitude in a very simple manner: the single spin terms $d\sigma_{UT}^I$, $d\sigma_{UL}^I$ and $d\sigma_{UT}^I$ are linear in the imaginary parts of the Compton form factors, i.e. to $\mathrm{Im}\,\mathcal{H}$, $\mathrm{Im}\,\mathcal{E}$, $\mathrm{Im}\,\tilde{\mathcal{H}}$ and $\mathrm{Im}\,\tilde{\mathcal{E}}$, whereas the unpolarized or double spin terms $d\sigma_{UU}^I$, $d\sigma_{LL}^I$ and $d\sigma_{LT}^I$ are linear in their real parts. Even better, one finds that in the interference terms one has *four* independent observables that allow one to separate the four Compton form factors. This is because for transverse polarization one can separate two terms that depend either on $\sin(\phi - \phi_S)$ or on $\cos(\phi - \phi_S)$, which respectively are maximal when the target spin is perpendicular to the hadron plane or in this plane. The different linear combinations are shown in table I.

We see that DVCS contains a multitude of observables that permit rather detailed access to the different GPDs. For meson production, the number of observables that can be computed in the Bjorken limit using collinear factorization is more limited: in fact one only has the unpolarized $\gamma^* p$ cross section and the single spin asymmetry for transverse proton polarization. Table II shows the corresponding bilinear combinations of meson production form factors, which are integrals over GPDs defined in a similar way as for Compton scattering [30]. Note that the relevant phase between form factors is important here: the term $\mathrm{Im}(\mathcal{E}_M^* \mathcal{H}_M)$ is for instance small if $\mathcal{E}_M^*$ and $\mathcal{H}_M$ are individually large but have nearly equal complex phases.

* * *

It is a pleasure to thank the students of the school for the many good questions they asked, and Mauro Anselmino and his team for organizing such a wonderful school.

TABLE I. – *Linear combinations of Compton form factors in the DVCS-Bethe-Heitler interference terms. The electromagnetic form factors F_1 and F_2 are to be evaluated at momentum transfer t. An ellipsis indicates terms that come with one or more powers of ξ and thus are suppressed in a wide range of kinematics. Complete expressions can be found in [29, 30]*

target polarization	GPD combination
unpolarized	$F_1\mathcal{H} + \xi(F_1+F_2)\tilde{\mathcal{H}} - \frac{t}{4m^2}F_2\,\mathcal{E}$
longitudinal	$F_1\tilde{\mathcal{H}} + \xi(F_1+F_2)\mathcal{H} - \left[\frac{\xi}{1+\xi}F_1 + \frac{t}{4m^2}F_2\right]\xi\tilde{\mathcal{E}} + \dots$
transverse $\propto \sin(\phi-\phi_S)$	$F_2\mathcal{H} - F_1\,\mathcal{E} + \dots$
transverse $\propto \cos(\phi-\phi_S)$	$F_2\tilde{\mathcal{H}} - F_1\;\xi\tilde{\mathcal{E}} + \dots$

TABLE II. – *Combinations of meson production form factors for the leading terms in the cross section at large Q^2.*

meson	target polarization	GPD combination
vector	unpolarized	$\lvert\mathcal{H}_M\rvert^2 - \frac{t}{4m^2}\lvert\mathcal{E}_M\rvert^2 - \xi^2\,\lvert\mathcal{H}_M+\mathcal{E}_M\rvert^2$
	transverse $\propto \sin(\phi-\phi_S)$	$\mathrm{Im}(\mathcal{E}_M^*\mathcal{H}_M)$
pseudoscalar	unpolarized	$(1-\xi^2)\,\lvert\tilde{\mathcal{H}}_M\rvert^2 - \frac{t}{4m^2}\,\lvert\xi\tilde{\mathcal{E}}_M\rvert^2 - 2\xi\,\mathrm{Re}(\xi\tilde{\mathcal{E}}_M^*\tilde{\mathcal{H}}_M)$
	transverse $\propto \sin(\phi-\phi_S)$	$\mathrm{Im}(\xi\tilde{\mathcal{E}}_M^*\tilde{\mathcal{H}}_M)$

REFERENCES

[1] JI, X.-D., *J. Phys. G*, **24** (1998) 1181 [hep-ph/9807358].
[2] GOEKE, K., POLYAKOV, M. V. and VANDERHAEGHEN, M., *Prog. Part. Nucl. Phys.*, **47** (2001) 401 [hep-ph/0106012].
[3] DIEHL, M., *Phys. Rept.*, **388** (2003) 41 [hep-ph/0307382].
[4] BELITSKY, A. V. and RADYUSHKIN, A. V., *Phys. Rept.*, **418** (2005) 1 [hep-ph/0504030].
[5] BOFFI, S. and PASQUINI, B., *Riv. Nuovo Cim.*, **30** (2007) 387 [arXiv:0711.2625].
[6] COLLINS, J. C., FRANKFURT, L. and STRIKMAN, M., *Phys. Rev. D*, **56** (1997) 2982 [hep-ph/9611433].
[7] COLLINS J. C., hep-ph/9907513.
[8] COLLINS J. C., *Foundations of perturbative QCD* (CUP, Cambridge) 2011.
[9] LIBBY S. B. and STERMAN G. F., *Phys. Rev. D*, **18** (1978) 4737.
[10] JAFFE, R. L., hep-ph/9602236.
[11] RADYUSHKIN, A. V., *Phys. Rev. D*, **56** (1997) 5524 [hep-ph/9704207].
[12] MÜLLER, D. *et al.*, *Fortsch. Phys.*, **42** (1994) 101 [hep-ph/9812448].
[13] BURKARDT, M. and SCHNELL, G., *Phys. Rev. D*, **74** (2006) 013002 [hep-ph/0510249].
[14] MUSATOV, I. V. and RADYUSHKIN, A. V., *Phys. Rev. D*, **61** (2000) 074027 [hep-ph/9905376].
[15] KUMERIČKI, K., MÜLLER, D. and PASSEK-KUMERIČKI, K., *Nucl. Phys. B*, **794** (2008) 244 [hep-ph/0703179].
[16] KUMERIČKI, K. and MÜLLER, D., arXiv:1008.2762.

[17] Ji, X.-D., *Phys. Rev. Lett.*, **78** (1997) 610 [hep-ph/9603249].
[18] Hägler, Ph., *Phys. Rept.*, **490** (2010) 49 [arXiv:0912.5483].
[19] Burkardt, M., *Int. J. Mod. Phys. A*, **18** (2003) 173 [hep-ph/0207047].
[20] Diehl, M., *Eur. Phys. J. C*, **25** (2002) 223; Erratum ibid. **31** (2003) 277 [hep-ph/0205208].
[21] Pire, B., Szymanowski, L. and Wagner, J., *Phys. Rev. D*, **83** (2011) 034009 [arXiv:1101.0555].
[22] Diehl, M. and Kugler, W., *Eur. Phys. J. C*, **52** (2007) 933 [arXiv:0708.1121].
[23] Vanderhaeghen, M., Guichon. P. A. M. and Guidal, M., *Phys. Rev. D*, **60** (1999) 094017 [hep-ph/9905372].
[24] Goloskokov, S. V. and Kroll, P., *Eur. Phys. J. C*, **53** (2008) 367 [arXiv:0708.3569].
[25] Anikin, I. V. and Teryaev, O. V., *Phys. Rev. D*, **76** (2007) 056007 [arXiv:0704.2185].
[26] Polyakov, M. V. and Weiss, C., *Phys. Rev. D*, **60** (1999) 114017 [hep-ph/9902451].
[27] Diehl, M. and Ivanov, D. Yu., *Eur. Phys. J. C*, **52** (2007) 919 [arXiv:0707.0351].
[28] Bacchetta, A. D'Alesio, U., Diehl, M. and Miller, C. A., *Phys. Rev. D*, **70** (2004) 117504 [hep-ph/0410050].
[29] Belitsky, A. V., Müller, D. and Kirchner, A., *Nucl. Phys. B*, **629** (2002) 323 [hep-ph/0112108].
[30] Diehl, M. and Sapeta, S., *Eur. Phys. J. C*, **41** (2005) 515 [hep-ph/0503023].